

EFFECTS OF SHIELDING ON PROPERTIES OF EDDY CURRENT PROBES WITH FERRITE  
CUP CORES

S. N. Vernon and T. A. O. Gross\*

Naval Surface Weapons Center, Silver Spring, MD 20903-5000

\*T. A. O. Gross, Inc., Lincoln, MA 01773-4116

INTRODUCTION

In eddy current inspection the ability to detect small defects depends on the sensitivity of the system and on the relative sizes of the probe and the defect. To detect defects on the opposite surface the probe radius should be at least as great as the thickness of the material. This limits the sensitivity to small defects that can be achieved by decreasing the probe size. Assuming the instrumentation is a given, further sensitivity can be achieved by improving the sensitivity of the probe itself.

Probe sensitivity depends on the coupling between the probe and the test material. Coupling is illustrated by the normalized impedance diagram (Fig. 1). Normalized reactance ( $X_n$ ) is the ratio of the reactance of the probe in contact with the material ( $\omega L_c$ ) to the reactance of the probe in air ( $\omega L_a$ ). Normalized resistance is the difference between the resistance of the probe on the material and the resistance in air divided by  $\omega L_a$ . Sensitivity can be described in terms of the coupling coefficient  $K$  where  $K^2 = 1 - X$ . The quantity  $X$  is the value of the normalized impedance where the extrapolated impedance curve intersects the reactance axis [1] (see Fig. 1). The coupling coefficient is proportional to the percentage of the total flux which links with the test material.

A number of factors affect the coupling coefficient. The most obvious is the separation between the probe and the test material (lift-off) as illustrated in Figure 1. Even with zero lift-off a coupling coefficient of 0.89 ( $X = .2$ ) would be excellent. Probe type [1] and distribution of windings [2] also affect probe sensitivity. Shielding can improve coupling by forcing into the test material some of the flux that would otherwise link within the coil itself.

This paper describes the effects of shielding on the sensitivity, or coupling, of a ferrite cup, or pot, core probe. Two types of shielding were investigated: self-shielding which results from skin effects in adjacent turns of the wire forming the coil and imposed shielding consisting of highly conductive metal on those surfaces of the cup which are not in contact with the test material. Bailey [3] and Ellsberry and Bailey [4] have reported on the characteristics of ferrite cylindrical core probes with imposed shielding. Gross [5] has investigated the effects of toroidal core probes with imposed shielding both on field intensity as a

function of distance from the probe face and on coupling. The cup core probe was selected for this investigation because even without shielding it appears to offer better coupling than either cylindrical or toroidal core probes.

### SELF-SHIELDING

The normalized impedance diagrams shown in Figure 2 illustrate the shielding that can be achieved using thick wire\*. The inner curve was generated by a probe having 15 turns of AWG #32 wire which has a diameter of 0.2 mm. It should be noted that the normalized impedance values for a carbon/carbon 3-D weave material ( $\rho \approx 900 \mu\Omega \text{ cm}$ ) fall on the same curve as the values for aluminum ( $\rho \approx 6 \mu\Omega$ ), as would be expected from theory. [6]. The lower curve was generated with a probe having 15 turns of #20 wire (diameter of 0.8 mm). At about 16 KHz the slope of the curve begins to change and the coupling improves with increasing frequency.

The curves in Figure 3 show those values of the probe inductance in air, normalized with respect to that inductance at 1 KHz, which are associated with each point on the lower portions of the impedance diagrams for the two probes. The impedance diagram for the #32 wire probe shows no change in slope and no change in the inductance of the probe in air. In contrast, the impedance curve for the #20 wire probe has a change in slope and the normalized inductance begins to decrease at a frequency slightly lower than the frequency at which the change in slope in the impedance curve becomes evident.

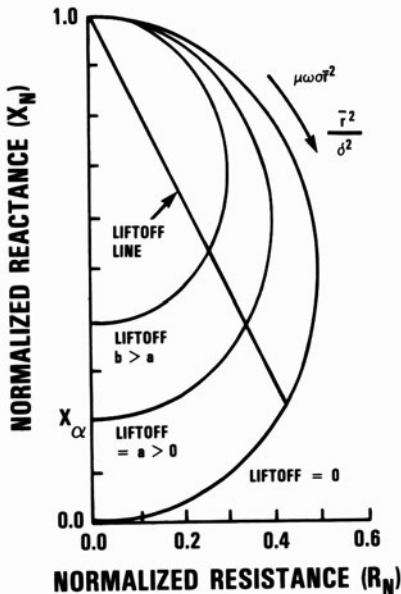


Fig. 1. Normalized impedance diagram showing the effects of lift-off, conductivity ( $\sigma$ ), frequency ( $\omega$ ), mean coil radius ( $r$ ), and skin depth ( $\delta$ ) for an idealized case.

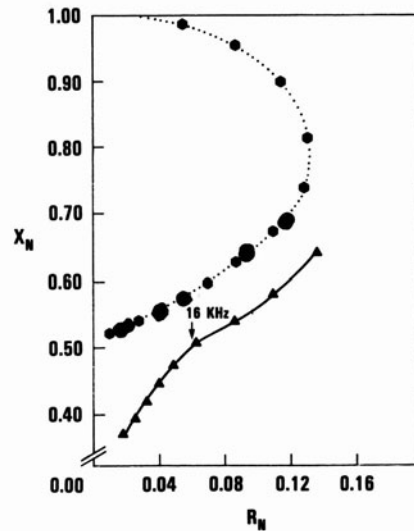


Fig. 2. Impedance diagrams for a probe wound with #32 wire (....) and for a #20 wire probe (--). Test materials: aluminum,  $\rho = 6 \mu\Omega \text{ cm}$  (● and ▲); carbon/carbon,  $\rho = 900 \mu\Omega$  (●).

\* All the probes described in this paper had an outside diameter of 3.6 cm. Similar results were obtained with probes as small as 0.8 cm.

The inductance of the probe in air is a measure of the mutual inductance among the turns in the coil. It is our hypothesis that as the frequency increases to a point where the skin depth in the wire approaches the radius of the wire, the flux associated with each turn in the coil no longer penetrates adjacent turns; there is mutual shielding in the coil. This reduces the mutual coupling and the inductance of the coil is slightly reduced. This mutual shielding has two effects. First, the flux that was linking within the coil is pushed into the surrounding ferrite and the test material, thereby increasing the coupling coefficient. Second, the mutual coupling and, consequently, the coil inductance, is slightly reduced. This reduction in coil inductance is not directly reflected in the change in slope of the impedance curve because the reactance is normalized with respect to both the frequency and the inductance. If the change in slope were a direct reflection of the decrease in probe inductance, the slope would change in the opposite direction.

Figure 4 shows the impedance curves and corresponding normalized inductance curves for a probe made with #22 wire (diameter = 0.6 mm) as well as those for the #20 wire probe. The change in slope in the impedance curve for the #22 wire probe appears at about 40 KHz. The inductance, again, begins to decrease at a slightly lower frequency.

The frequency at which the skin depth in copper is equal to the wire radius is given in Table I for the three gauges of wire investigated. For #20 and #22 wire, the changes in slope were observed at 16 KHz and 40 KHz respectively. The curves were generated by increasing the frequency in octave steps, consequently the frequency at which the slope change occurs cannot be identified more accurately than about  $\pm 75\%$ . Given this uncertainty, there is good agreement with the values given in the table - except for the #32 wire. The effect on the curves for the #22 wire probe is less than the effect on the #20 wire. It is reasonable that the thinner the wire the less the shielding effect. #32 wire is simply too thin to prove an observable effect.

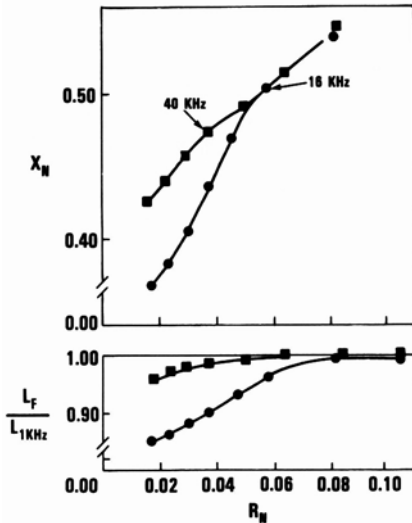


Fig. 3. Impedance diagrams and values of normalized inductance  $L_f/L_1$  KHz) associated with each impedance value for #32 wire probe (●) and #20 wire probe (▲).

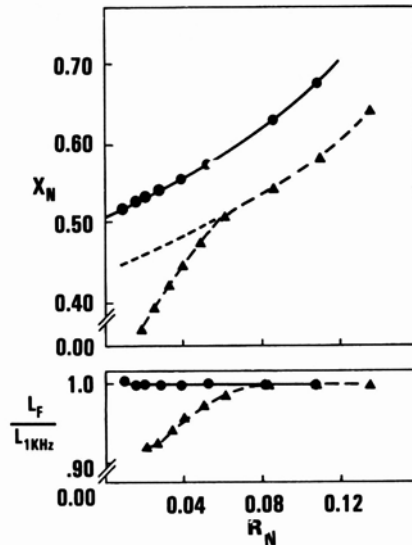


Fig. 4. Impedance diagrams and associated normalized inductance values for #20 wire probe (●) and for #22 wire probe (▲).

TABLE I

Frequency at which the skin depth in Cu = wire radius

WIRE GAUGE	WIRE RADIUS (in.)	FREQ. AT WHICH SKIN DEPTH = RADIUS (KHz)
32	0.004	422
22	0.0125	43
20	0.016	26

Figure 5 shows the #20 wire probe impedance curves for aluminum, tantalum, titanium alloy, and carbon/carbon. The curve for each material deviates from the unshielded curve between about 16 and 40KHz. The deviation is much less obvious in the upper portion of the curve, but it is present. It is generally assumed that the impedance curve is independent of the resistivity of the test material, as was the case for the #32 wire probe curve.

The benefits of increased sensitivity resulting from self-shielding effects can be applied to the inspection of any material. In the inspection of aluminum, for example, frequencies above 40 KHz are normally used. Since aluminum components inspected by eddy current methods are generally quite thin, smaller probes are used than those considered here. As a consequence the curve for aluminum could correspond to the curve for carbon/carbon where the benefits of self-shielding occur in the useable [1] mid range of the curve.

If a very small probe is required it may not be possible to use thick wire and still have enough turns to provide the impedance required by the instrumentation. Similar shielding effects can be achieved with imposed shielding.

#### IMPOSED SHIELDING

Shielding, in the form of metal sheets or electro-deposited metal, can be placed on any or all of the five surfaces: a, b, c, d, and e, shown in Figure 6. The method for the electro-deposition of copper is described in reference 5. Experimentation has indicated [5] that the shielding should be electrically insulated from the ferrite. Copper sheeting having a thickness of 0.005 inches is convenient to use on large probes. Since it is difficult to accurately cut small pieces of the sheeting, it may be more convenient to use electro-deposition for small probes. Any high conductivity metal will suffice. Silver offers some improvement but may not be worth the additional cost. It is important that there be a gap in the circumference of the shielding to avoid the shorted-turn effect. [5]

The effects typical of imposed shielding are shown (Fig. 7) for the #32 wire probe. The solid curve is the unshielded impedance diagram for both carbon/carbon and aluminum. The dashed line is the aluminum impedance curve for the same coil placed in a ferrite cup core with copper deposited on the 5 surfaces. The dotted line is the corresponding curve for carbon/carbon. Probe sensitivity, or coupling, begins to show an improvement over the unshielded probe at about 16 to 32 KHz. Below this frequency the coupling is worse for the shielded than for the unshielded probe. This effect was found to be independent of number of turns and probe size. The reason for this effect is not well understood.

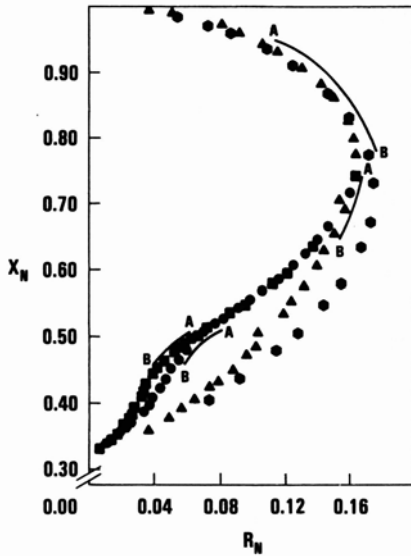
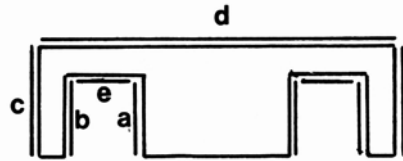


Fig. 5. Impedance diagrams for #20 wire probe on aluminum (■) tantalum (●  $\rho = 13 \mu\Omega \text{ cm}$ ), titanium alloy (▲  $\rho = 171 \mu\Omega \text{ cm}$ ) and carbon/carbon (◆). A = 16 KHz, B = 40 KHz

Fig. 6. Cross-section of a ferrite cup core showing surfaces that can be shielded.



Again the benefits of shielding can be achieved for the inspection of high conductivity metals by using a smaller probe at frequencies above 16 KHz.

Some further increase in coupling can be achieved by adding imposed shielding to probes which already provide self-shielding. Figure 8 illustrates this effect on the impedance curve of the #20 wire probe. The normalized inductance of the shielded probe in air begins to decrease immediately, agreeing with the evidence that shielding has an effect, albeit an unwanted one, at very low frequencies.

Reference 5 reports the effects of imposed shielding on the intensity of the field as a function of distance, both along the probe axis and normal to the axis. Within a distance of one radius normal to the probe face, the field was stronger for the shielded probe. At a distance of five radii the field was stronger for the unshielded probe.

A cursory investigation indicated (Figure 9) that when the windings filled the cup of the core, shielding only surface b resulted in a less negative effect on coupling at low frequencies and improved coupling at a lower frequency.

## CONCLUSIONS

A significant improvement in probe sensitivity can be achieved through the use of shielding. Self-shielding results from the use of larger diameter wire when the operating frequencies are greater than the frequency at which the skin depth in the wire is greater than the radius of the wire.

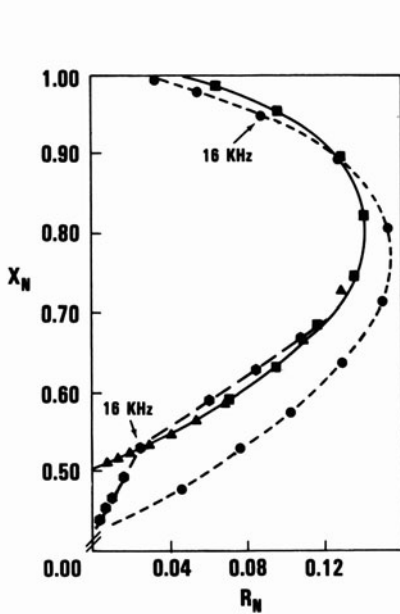


Fig. 7. Impedance diagrams for the #32 wire probe:  $\blacksquare$  unshielded on carbon/carbon,  $\blacktriangle$  unshielded on aluminum,  $\bullet$  shielded on c/c,  $\bullet$  shielded on Al.

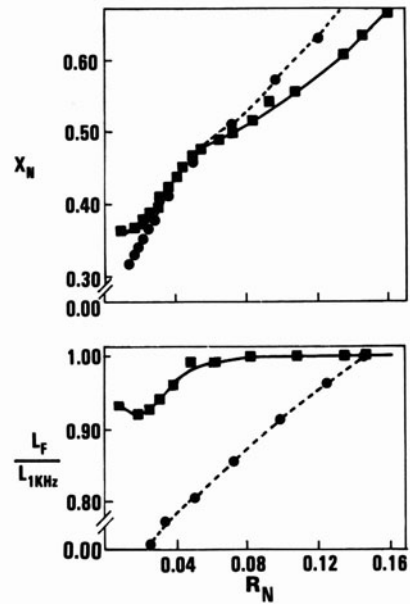


Fig. 8. Aluminum impedance diagrams and associated values of normalized inductance for the #20 wire probe with no imposed shielding ( $\blacksquare$ ) and with imposed shielding ( $\bullet$ ).

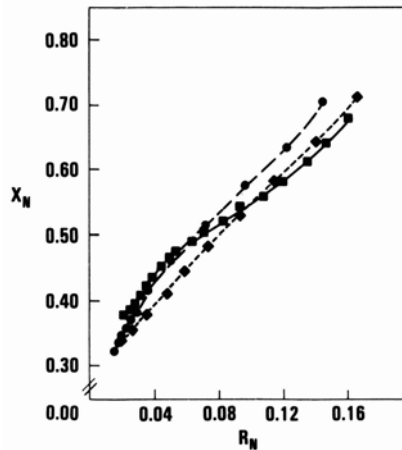


Fig. 9. Impedance diagrams for the #20 wire probe with no imposed shielding ( $\blacksquare$ ), with deposited shielding on 5 surfaces ( $\bullet$ ), and with shielding only on surface b ( $\blacklozenge$ ).

Theoretical modeling should take into account the effects of self-shielding. In the absence of self-shielding the coupling coefficient is independent of the resistivity of the test material. For a given probe normalized impedance depends on the quantity  $\mu\sigma\omega r^2$  where  $\mu$  is the relative permeability,  $\sigma$  is the conductivity,  $\omega$  is the angular frequency and  $r$  is the mean radius of the coil. When the frequency and wire size are such that there is a self-shielding effect, the normalized probe impedance has an additional dependency on material conductivity and frequency. The

impedance associated with the material affects the flaw response, so skin effects in the wire should be considered in flaw inversion modeling.

Imposed shielding can increase the sensitivity of probes that are too small to contain the necessary number of turns of larger diameter wire.

#### REFERENCES

1. Vernon, S.N., "Probe Properties Affecting the Eddy Current NDI of Graphite Epoxy," Review of Progress in Quantitative Nondestructive Evaluation, Vol 5B, Donald O. Thompson and Dale E. Chementi, Ed., Plenum Press, New York, (pub 1986), pp 1113-1123.
2. Smith, S.H. and C.V. Dodd, "Optimization of Eddy Current Measurements of Coil to Conductor Spacing," Materials Evaluation, Vol. 33, No. 12, Dec 1975, pp 279-283, 292.
3. Bailey, D.M., "Shielded Eddy Current Probes," Materials Evaluation, Vol. 41, Jun 1983, pp 776-777.
4. Elsberry, R.T. and D.M. Bailey, "Characterization of Shielded Eddy Current Probes," Materials Evaluation, Vol. 44, No. 8, July 1986, pp 984-988.
5. Gross, T.A.O., "Final Report: Eddy Current Inspection of Graphite Epoxy Composites," Final Report, Naval Surface Weapons Center Contract No. N60921-85-C-0257, 7 Apr 1986.
6. Libby, H.L., Introduction to Electromagnetic Test Methods (New York: John Wiley and Sons, Inc., 1971), pp 122-179.